Deposition of Submicron Aerosol Particles in Turbulent and Transitional Flow

Manabu Shimada and Kikuo Okuyama
Dept. of Chemical Engineering, Hiroshima University, Higashi-Hiroshima 724, Japan

Masahito Asai
Dept. of Aerospace Engineering, Tokyo Metropolitan Institute of Technology, Hino 191, Japan

Brownian and turbulent diffusive deposition of submicron aerosol particles from pipe flow is studied experimentally and theoretically. A theoretical model for evaluating the turbulent diffusive deposition is presented in which a turbulent flow in a circular pipe is numerically calculated based on the k-ϵ turbulent flow model and deposition velocities are derived by solving the convection-diffusion equation. Deposition velocities of monodisperse aerosol particles, 0.01–0.04 μm in diameter, are obtained experimentally by measuring the decrease in the particle number concentration of an aerosol at two cross-sections of a circular test pipe through which the aerosol is flowing. The deposition velocities obtained when Re is larger than about 3,000 agree well with those predicted by the present analysis which are proportional to the 0.92nd power of Reynolds number and the 0.33rd power of Schmidt number. The particle deposition rates are measured when $1{,}000 \leq Re \leq 2{,}000$ suggest a transitional state for particle deposition which cannot be explained by the present analysis nor by the laminar pipe flow deposition theory.

Introduction

The deposition of fine particles from turbulent gas stream occurs, for example, during dry deposition of atmospheric aerosols and wall deposition of indoor aerosols. Aerosol deposition is also closely related to problems of microcontamination in various manufacturing industries. In the manufacturing process of LSIs, in which surface contamination due to particulate contaminants causes serious problems, downflow or laminar flow clean rooms and clean tunnels are used to obtain clean air containing very little dust. However, air flow in downflow clean rooms is not limited to laminar flow; air streams passing around obstacles, such as tables or manufacturing devices, or those induced by moving bodies can easily cause fluctuations in the air motion. Turbulent eddies in gas streams are also generated in the process gas contained in reaction chambers which undergoes gas exhaust and suction. In this case, particles attached to the chamber walls may be re-entrained into the gas and transported onto surfaces of materials by the strong fluctuating motion of the air flow.

Particle deposition from a turbulent gas flow is affected by diffusive transport and the relative motion of the particle with respect to the air due to particle inertia. The effect of turbulent flow on aerosol deposition has been studied by many researchers since Friedlander and Johnstone (1957). The main objective of the previous studies was to analyze deposition of particles that are large enough to arrive at a surface by inertial impaction, namely particles larger than several hundreds of nanometers.

Theoretical investigations of turbulent deposition are roughly classified into two approaches: one is the free-flight model first presented by Friedlander and Johnstone together with its modifications (Davies, 1966; Beal, 1970; Sehmel, 1970; Yoshioka et al., 1972; Sehmel, 1973; Forney and Spielman, 1974; Liu and Ilori, 1974; Wood, 1981) the other is based on the assumption that particles are transported toward a wall by periodic downward flowing air streams which are induced in

Correspondence concerning this article should be addressed to M. Shimada.

turbulent burst processes (Cleaver and Yates, 1975; Fichman et al., 1988).

Experimental investigations include measurements performed using turbulent air flow inside pipes, channels or wind tunnels. Most of the existing data are limited to micrometer sized particles and have been presented in terms of relaxation times which describe the magnitude of particle inertia. However, as stated by Papervergos and Hedley (1984), significant scatter is still found in the data reported by different investigators. The effect of particle inertia in a turbulent flow field is not well understood.

Deposition of submicron particles is increasingly important as a source of surface microcontamination. The deposition is dominated by turbulent diffusive transport which is another important mechanism in turbulent deposition. Previous experimental results are insufficient to give an accurate evaluation of turbulent diffusive deposition because deposition of micrometer size particles is simultaneously (or mainly) affected by particle inertia. There have been no reported experimental data on submicron particle deposition, which is considered to be mainly because of the following difficulties in practical techniques:

- ***Generation of Test Particles.*** It is difficult to generate ultrafine aerosol particles electrically uncharged and well defined in size continuously, stably and in high number concentration.

- ***Dilution of Aerosol.*** Dilution of a generated aerosol is needed to prepare a large amount of test aerosol flowing as a turbulent flow. It is quite difficult to obtain the test aerosol with a uniform particle distribution because sufficient mixing of the aerosol is required.

- ***Measurement of the Amount of Deposited Particles.*** Direct measurement of the amount of deposited particles is practically very difficult since the particles are not large enough to be detected easily by microscopes.

These difficulties are the reasons that most existing studies on particle deposition were limited to large, micrometer-sized particles or laminar flows. The contribution of the turbulent diffusive transport has not been fully evaluated and a clarification of the effect of turbulent flow is still required.

Fully developed turbulent or pure laminar flow fields have been examined in previous deposition experiments, but there is very little information on deposition in a transitional flow region. Our recent study (Shimada et al., 1991) investigated deposition in flows ranging from the laminar to the turbulent state, which is practically encountered in many situations, using flows in standard stirred tanks and suggested the existence of a transitional region for particle deposition.

The primary purpose of this study is to obtain deposition rates of submicron particles in a turbulent flow experimentally. The turbulent diffusive transport of particles onto a wall is investigated both experimentally and theoretically. The system considered in this study is an aerosol flowing in a circular pipe. A model calculation is firstly presented and demonstrated for diffusive transport of particles in turbulent flows. The properties of the flow are obtained by the low-Reynolds number k-ϵ turbulent model which has not been applied to investigate deposition of ultrafine particles. The flow properties are included in the convective-diffusion equation for particles, and the deposition rates of the particles are computed. An experimental setup to investigate the deposition is developed in which an evaporation-condensation aerosol generator, an ejector as an effective tool for aerosol dilution and a condensation nucleus counter for very fine particles are included. The deposition velocity onto the inner walls of a pipe is measured with monodisperse particles 0.01–0.04 μm in diameter. The effects of air flow rate and particle size are discussed by comparing the predicted values with the measurements. Finally, deposition rates in flow fields ranging from turbulent to transitional flow are presented.

Theoretical Analysis

Model describing deposition in turbulent pipe flow

The transport of aerosol particles flowing in a pipe is affected by both Brownian and turbulent diffusion of the particles, gravitational and inertial forces, and external forces such as electrical forces. Forces due to gravity and particle inertia, however, are generally negligible for particles smaller than 0.1 μm, and the deposition of such small particles is the objective of this study. The effect of external forces is also excluded in the present analysis. Consequently, particle deposition in a turbulent flow field is governed by Brownian diffusion and turbulence in the air stream. The transport of particles in a straight, circular pipe at steady state can therefore be described by:

$$\frac{1}{r}\frac{\partial}{\partial r}\left[r\,(D+D_E)\frac{\partial n}{\partial r}\right]=u\frac{\partial n}{\partial z} \tag{1}$$

where r and z are the radial and axial coordinates, respectively, n is the particle number concentration, and D_E is the turbulent diffusion coefficient of the particles. The local air velocity in the axial direction, $u(r)$, is the time-average velocity. The Brownian diffusion coefficient, D, in the above equation is given by the following Stokes-Einstein equation:

$$D=\frac{\kappa TC_c}{3\pi\mu d_p} \tag{2}$$

where κ is the Boltzmann constant, T is the absolute temperature, μ is the air viscosity, d_p is the particle diameter, C_c is the Cunningham correction factor (Davies, 1945). Equation 1 will be taken as the basic equation describing the particle distribution in a turbulent pipe flow.

The magnitude of Sc (the Schmidt number), which denotes the ratio of the kinematic viscosity of the air to the Brownian diffusivity of the particles, is 10^2–10^4 for the particles considered in this study. This suggests that the rate of particle transport by Brownian diffusion is extremely small compared with transport of fluid momentum. The distribution of particles in a pipe is, therefore, expected to be nearly uniform throughout a section of the pipe except in a very thin layer near the pipe walls, where the particle concentration decreases rapidly. Analysis of a turbulent flow is therefore performed using a $k-\epsilon$ turbulence model which can be applied to the phenomena occurring near the wall and which is called the low-Reynolds-

number model. The model for fully developed, incompressible turbulent air flow in a circular pipe is given by Jones and Launder (1972) as:

$$\frac{1}{r}\frac{d}{dr}\left[r(\nu+\nu_t)\frac{du}{dr}\right]=\frac{1}{\rho}\frac{dP}{dz}=\text{const.} \tag{3}$$

$$\frac{1}{r}\frac{d}{dr}\left[r\left(\nu+\frac{\nu_t}{\sigma_k}\right)\frac{dk}{dr}\right]+\nu_t\left(\frac{du}{dr}\right)^2-\epsilon-2\nu\left(\frac{dk^{1/2}}{dr}\right)^2=0 \tag{4}$$

$$\frac{1}{r}\frac{d}{dr}\left[r\left(\nu+\frac{\nu_t}{\sigma_\epsilon}\right)\frac{d\epsilon}{dr}\right]+C_1f_1\nu_t\frac{\epsilon}{k}\left(\frac{du}{dr}\right)^2-C_2f_2\frac{\epsilon^2}{k}+2\nu\nu_t\left(\frac{d^2u}{dr^2}\right)^2=0 \tag{5}$$

where k is the turbulent energy, ϵ is the local energy dissipation, ρ, ν and P are the density, kinematic viscosity and pressure of the air. ν_t is the eddy kinematic viscosity of the air and given by:

$$\nu_t=C_\mu f_\mu\frac{k^2}{\epsilon} \tag{6}$$

The constants C_1, C_2, C_μ, σ_k, σ_ϵ and values of f_1, f_2, f_μ are given as follows:

$$C_1=1.55,\quad C_2=2.0,\quad C_\mu=0.09,$$
$$\sigma_k=1.0,\quad \sigma_\epsilon=1.3,$$
$$f_1=1,\quad f_2=1-0.3\exp(-R_t^2),\quad f_\mu=\exp\{-2.5/(1+R_t/50)\},$$
$$R_t=k^2/\nu\epsilon \tag{7}$$

The pressure drop term in Eq. 3 is calculated by the Fanning's equation and the friction factor from the Blasius' equation as:

$$dP/dz=4f\rho\bar{u}^2/(4R) \tag{8}$$

$$f=0.0791\mathrm{Re}^{-0.25} \tag{9}$$

where $\bar{u}$ is the average velocity over a cross-section of the pipe, R is the pipe radius, and Re is the Reynolds number defined as $Re=2R\bar{u}/\nu$.

The boundary conditions for Eqs. 3-5 are as follows:

$$\begin{aligned} &du/dr=dk/dr=d\epsilon/dr=0 && \text{at } r=0\\ &u=k=\epsilon=0 && \text{at } r=R \end{aligned} \tag{10}$$

The calculation domain is a section of the pipe. In the calculation procedure, the radial coordinate is divided into a nonuniform mesh in which the grid size becomes smaller as the pipe wall is approached. u, k, ϵ, and ν_t are evaluated by converting Eqs. 3-5 into finite difference equations and solving them numerically. Accurate results were obtained with a mesh of 500 grid points along a pipe radius. The smallest mesh interval was set at the surface of the pipe wall and was about 10^{-8} m. Successive solutions of the simultaneous equations were produced until all the values of u, k, and ϵ converged at every grid point. After convergence the local eddy diffusivity ν_t was recalculated from Eq. 6.

The turbulent diffusion coefficient of aerosol particles, D_E, appearing in Eq. 1 was assumed to have the form

$$D_E=\nu_t/Sc_t \tag{11}$$

where Sc_t is the turbulent Schmidt number. The value of Sc_t, which equals the ratio of momentum to mass transfer due to turbulent eddies, will be a function of particle mass and size since motion of a particle can no longer follow the motion of the fluid as the mass and the size of the particle become large. The relationship between ν_t and D_E is not clear because the fluctuating motion of the particles is affected by the interaction of the particles with the turbulent eddies and this is not fully understood. In this analysis, the particles are assumed to follow the fluid motion perfectly since the effect of particle inertia was estimated to be negligible, and the rate of particle transfer was postulated to be equal to that of momentum transfer. That is, Sc_t is set to be 1.

The distribution of the turbulent diffusion coefficient was substituted into Eq. 1 and this equation was then solved numerically using a finite difference method. After obtaining the distribution of the particle concentration along the pipe radius, the deposition velocity was calculated using

$$v_d=-\frac{D}{n_C}\frac{\partial n}{\partial r}\bigg|_{r=R-d_p/2} \tag{12}$$

where n_C is the concentration at the center of the pipe.

Results of model calculations for turbulent deposition

Figure 1 shows the dependence of D_E on the dimensionless distance from the pipe wall surface, y^+ $(=yu*/\nu,\ y=R-r,\ u*=\bar{u}(f/2)^{0.5})$. The turbulent diffusion coefficient decreases as the surface is approached, indicating that the particle transport by turbulent eddies is attenuated near the wall surface. The slope of the graph indicated that the value of D_E is nearly

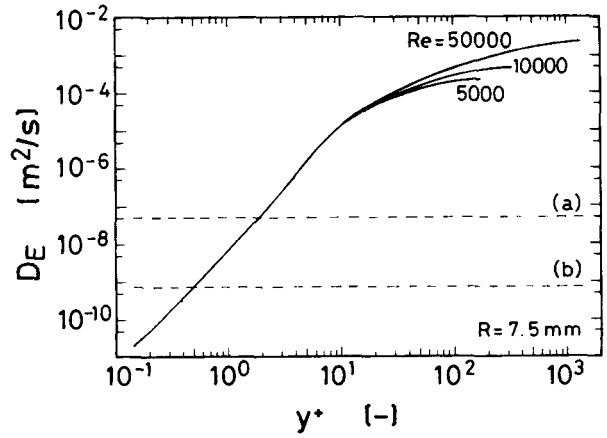

Figure 1. Change in turbulent diffusion coefficient, D_E, with dimensionless distance from wall, y^+.

Dashed lines indicate Brownian diffusion coefficients for particles of 0.01 μm (a) and 0.1 μm (b) in diameter.

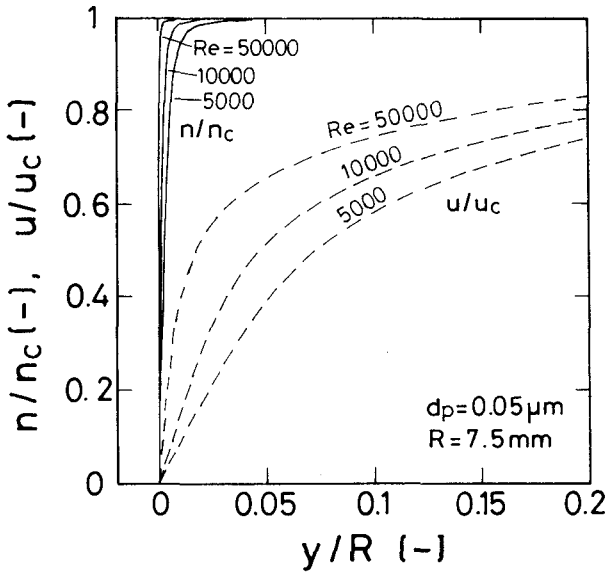

Figure 2. Distribution of the dimensionless particle concentration, n/n_C, and air flow velocity, u/u_c, against the dimensionless distance from wall, y/R.

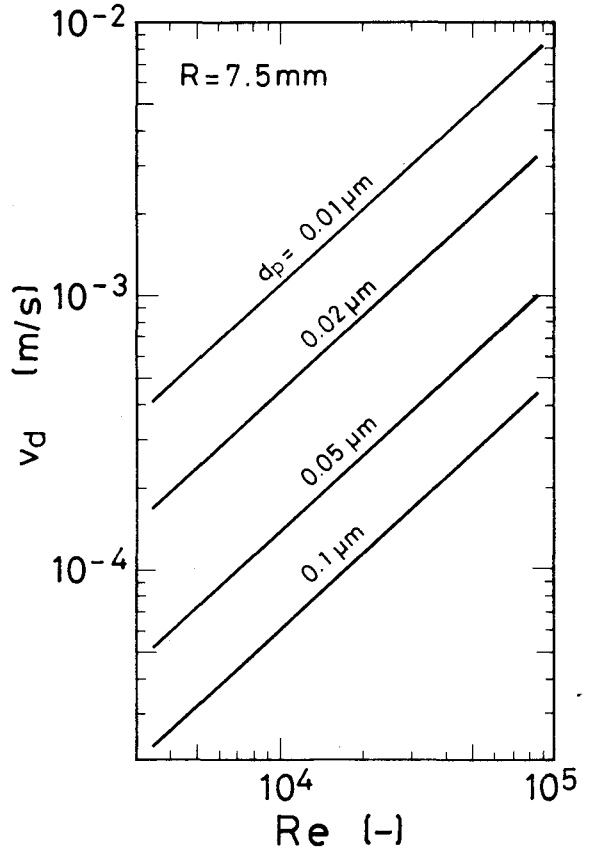

Figure 3. Change in the calculated deposition velocity, v_d, as a function of the Reynolds number, Re.

proportional to $(y^+)^3$ in the vicinity of the wall. The dashed lines in the figure correspond to the magnitude of the Brownian diffusion coefficient of particles 0.01 and 0.1 μm in diameter. Those lines suggest that the turbulent diffusive transport due to eddies in the mainstream dominates up to the point of intersection between the solid and dashed lines; the influence of Brownian diffusion is limited to the very thin region between the point of intersection and the wall surface.

Typical distributions of air velocity, u, and particle concentration, n, are shown in Figure 2. The abscissa is the dimensionless distance from the wall, the value of which is zero at the wall surface and unity at the center. The ordinates are the dimensionless particle concentration and air velocity which are both normalized by their maximum values at the central axis. Both the concentration and the velocity approach zero as the distance from the wall decreases, but the gradient of the particle concentration near the wall is much steeper than that of the air velocity. This means that the particle concentration boundary layer is much thinner than the air velocity boundary layer. The thickness of the concentration boundary layer is found to decrease with an increase in the Reynolds number in the same manner as the velocity boundary layer.

Figure 3 shows examples of the deposition velocity v_d calculated under various conditions of particle size and air flow rate. At a constant particle size, the deposition velocity increases with Re because the concentration gradient near the wall ($\partial n/\partial y$) becomes larger (see Figure 2), and furthermore the value of v_d is proportional to the 0.92nd power of Re. The deposition velocity also increases when the particle size decreases, which is attributed to the higher Brownian diffusivity of the smaller particles.

A number of numerical calculations with various particle sizes, air flow rates, and pipe diameters showed that all the calculations could be correlated in terms of the dimensionless parameters Re and Sc as:

$$Sh = 9.2 \times 10^{-3} Re^{0.92} Sc^{0.33} \tag{13}$$

where the Sherwood number or dimensionless deposition velocity, Sh, is defined as $2Rv_d/D$. This equation is readily transformed to give the deposition velocity directly as:

$$v_d = 1.2 \times 10^{-4} Re^{0.92} D^{0.67}/R \tag{14}$$

where the kinematic viscosity of air, ν, is substituted by 1.5×10^{-5} m^2/s.

Although the general form of Eq. 13, $Sh = A\,Re^b Sc^c$, has been widely adopted in the existing studies concerned with aerosol deposition in pipes, several sets of values have been reported for the constant and the exponents appearing in the formula. As a representative example of the equations that express the turbulent diffusive deposition velocity, the equation presented by Friedlander (1977) is as follows:

$$Sh = 4.2 \times 10^{-2} Re f^{1/2} Sc^{1/3} \tag{15}$$

This equation was based on the experimental data for the turbulent diffusive mass transfer in aqueous solution where the turbulent diffusion coefficient in the viscous sublayer was correlated to be proportional to y^3. Substitution of Eq. 9 into Eq. 15 gives the deposition velocity as:

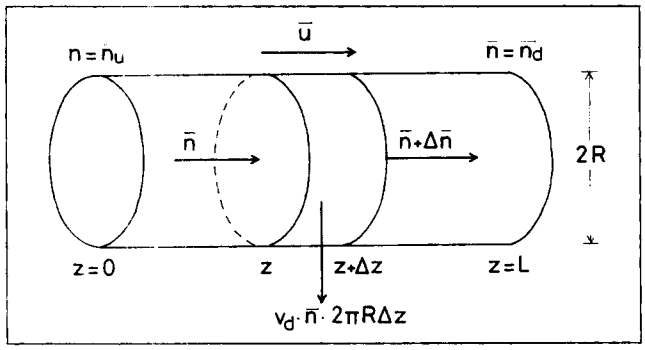

Figure 4. Relationship between the change in the particle concentration, $\bar{n}$, and the deposition velocity, v_d, in a circular pipe.

$$v_d = 1.5 \times 10^{-4} Re^{0.88} D^{0.67}/R \tag{16}$$

The experimental portion of this study examines the appropriateness of Eqs. 13 or 14 and in particular the values of the constants derived in the numerical simulations.

Concentration change in the axial direction of pipe

The change in the particle concentration in the axial direction (penetration) is predicted using the deposition velocity. The relationship between the penetration and the deposition velocity is illustrated in Figure 4. The number of particles flowing through a pipe section z is $\pi R^2 \bar{u}\,\bar{n}$ per unit time, where $\bar{n}$ is the average concentration over a section of the pipe. $\bar{n}$ is very close to the concentration at the pipe center, n_C, because the radial distribution of particles is uniform except in the very thin layer close to the wall as shown in Figure 2. Thus, the number of particles, $-\Delta\bar{n}$, lost due to deposition within a small section (length Δz) per unit time is $2\pi R\Delta z n_C v_d \approx 2\pi R\Delta z \bar{n} v_d$ from the area of surface where deposition is occurring. Since the number of particles passing through the section $z+\Delta z$ is given by $(\pi R^2\bar{u})\,(\bar{n}+\Delta z d\bar{n}/dz)$, change in the concentration $\bar{n}$ obeys

$$\frac{d\bar{n}}{dz} = -\frac{2v_d}{R\bar{u}}\bar{n} \tag{17}$$

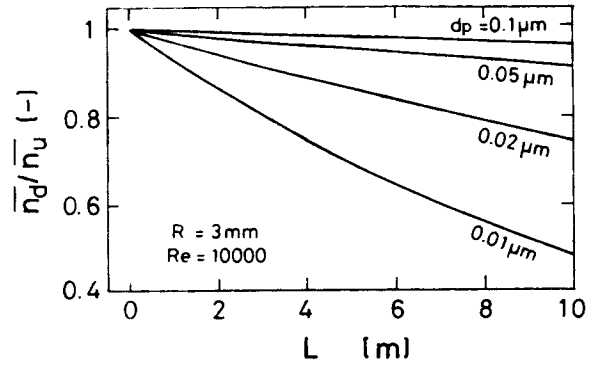

Figure 5. Ratio of particle concentrations at two sections separated by distance *L*.

Consequently, the penetration of particles between the two cross-sections is given by:

$$\frac{\bar{n}_d}{\bar{n}_u} = \exp\left(-\frac{2v_{dav}L}{R\bar{u}}\right) \tag{18}$$

and

$$v_{dav} = \frac{1}{L}\int_{z_u}^{z_d} v_d dz \tag{19}$$

where $\bar{n}_u$ and $\bar{n}_d$ are the average concentrations at two sections ($z=z_u$ and $z=z_d$) separated by a distance L.

Concentration change for turbulent flow

Since the deposition velocity for fully developed flow does not depend on the axial position z as demonstrated in the previous section, v_{dav} is equal to v_d and Eq. 18 becomes

$$\frac{\bar{n}_d}{\bar{n}_u} = \exp\left(-\frac{2v_d L}{R\bar{u}}\right) \tag{20}$$

Figure 5 shows examples of the calculation from Eqs. 14 and 20. As expected, the penetration of particles decreases as the distance L increases. The higher deposition rates of small particles also results in decreased penetration.

Concentration change for laminar flow

Deposition in flows in a transitional state is also investigated in this study. Since a theoretical evaluation of the deposition in a transitional flow is not available in the existing literature, the solution by Gormley and Kennedy (1949) for deposition from laminar pipe flows is briefly described here for comparison with the low flow rate experiments. The concentration change for the aerosol particles in a developed laminar flow is given by

$$\bar{n}(z)/n_0 = 0.8191\exp(-3.657\beta) + 0.0975\exp(-22.3\beta) + 0.0325\exp(-57\beta) + \ldots \quad (\beta \geq 0.0312)$$

$$\bar{n}(z)/n_0 = 1 - 2.56\beta^{2/3} + 1.2\beta + 0.177\beta^{4/3} + \ldots \quad (\beta < 0.0312)$$

$$\beta = Dz/\bar{u}R^2 \tag{21}$$

where n_0 is the uniform concentration prevailing over the pipe section of the axial position $z=0$. The local deposition velocity, $v_d(z)$, is calculated by solving this equation and Eq. 17. The average deposition velocity over the sections $z=z_u$ and $z=z_d$ can then be obtained from Eq. 19.

Experimental Apparatus and Procedure

Figure 6 shows a schematic diagram of the experimental apparatus. Dry, clean air supplied by a compressor and an absolute filter flows through an ejector. The aerosol preparation system consisting of an evaporation-condensation aer-

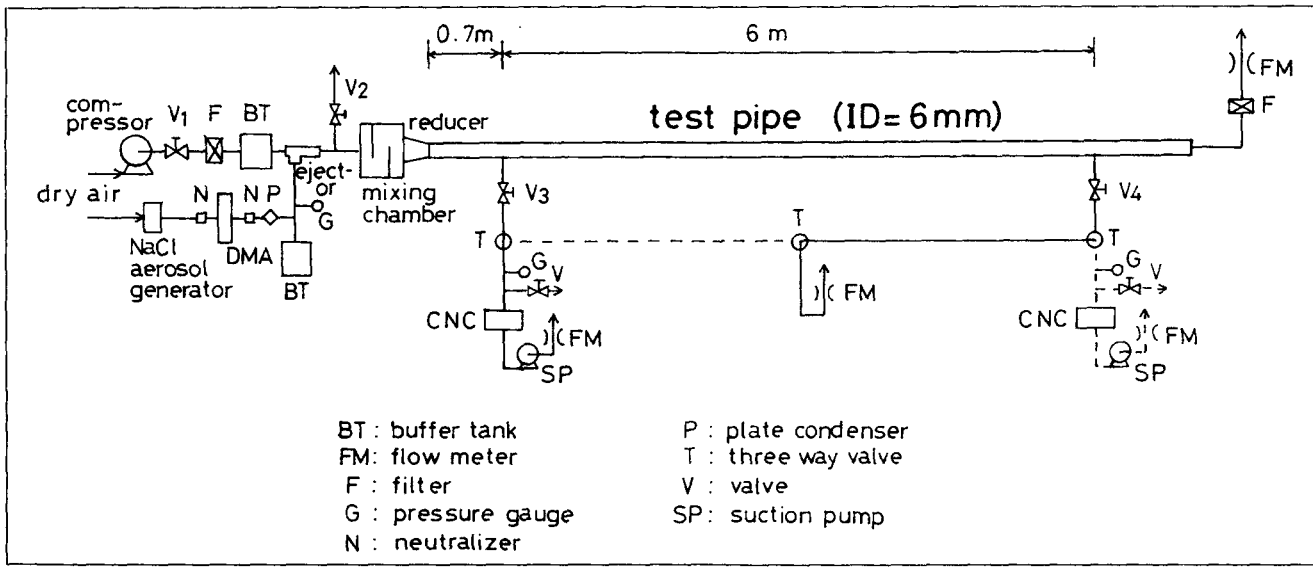

Figure 6. Experimental apparatus.

osol generator and a differential mobility analyzer (DMA) is almost the same as that reported in our experiment previously (Okuyama et al., 1984). This generator can quite stably produce ultrafine particles at a flow rate of 1.0×10^{-3} m^3/min, which have the geometric standard deviation of about 1.4 and the number concentration of 10^{11}-10^{14} particles/m^3. The geometric standard deviation of submicron aerosol particles classified by the DMA is less than 1.2, so that they can be treated as sufficiently monodisperse particles. The particles are then electrically neutralized and introduced into an electrical plate condenser to remove charged particles. The resulting uncharged particles are mixed with the air from a buffer tank by suction with the ejector in which immediate and sufficient mixing of the aerosol occurs without changing the air pressure in the aerosol preparation system considerably. The diameter of the particles ranges from 0.01 μm to 0.04 μm. The valve V_2 installed at the air exhaust prior to a mixing chamber adjusts the amount of aerosol being sucked. The diluted aerosol then flows through a reducer and into the straight test pipe.

The inner diameter of the copper test pipe, $2R$, is 6 mm. The flow rate of aerosol in the pipe is adjusted to be between 4.3×10^{-4} and 4.3×10^{-2} m^3/min, which corresponds to Reynolds numbers, Re, between 10^2 and 10^4.

The test pipe is equipped with two sampling taps spaced 6 m apart. The distance between the reducer outlet and the sampling tap at the upstream side is 0.7 m. The particle number concentration at a tap position is measured by a mixing-type condensation nucleus counter (CNC) (Kousaka et al., 1985). The amount of aerosol sampled by the CNC is varied between 4.3×10^{-4} and 10^{-3} m^3/min in accordance with the flow rate of the aerosol in the test pipe and the following sampling methods.

Two methods are adopted here for sampling the aerosol from the test pipe. The first method, Method i, is mainly used when the flow rate in the pipe is sufficiently large (more than ten times larger than the rate of air sampled by the CNC). In this case, when particles are sampled from one of the two taps, a portion of the aerosol is discharged from the other tap in the same flow rate as CNC's sampling flow rate. The flow through the test section is thereby maintained at a constant velocity. When the flow rate in the pipe is not much larger than the sampling air flow rate, the second method, Method ii, is adopted. In this method, all the aerosol flowing in the test pipe is discharged from one of the sampling taps by closing the other tap and the pipe outlet at the same time.

The penetration of particles is obtained from the concentration measured at the upstream side, $\bar{n}_u$, and that at the downstream side, $\bar{n}_d$. If the concentration change is due solely to particle deposition, the deposition velocity is readily determined by the following equation derived from Eqs. 18 or 20.

$$v_{dav} \text{ or } v_d = -(R\bar{u}/2L)\ln(\bar{n}_d/\bar{n}_u) \tag{22}$$

This equation is valid when coagulation of particle does not take place in the test section. Calculations in which the experimental conditions were taken into account (Appendix) showed that the change in the particle concentration due to particle coagulation can be neglected when particle concentration did not exceed about 4×10^{11} particles/m^3. On the other hand, the lowest concentration limit in the actual measurement is governed by the particle concentration measurement using the CNC. Practically, the concentration measurement becomes very difficult when concentration is less than about 10^6 particles/m^3. The particle concentration in the test pipe is therefore adjusted between 10^7 and 10^8 particles/m^3.

Results of Measurement and Comparison with Theoretical Calculations

Pressure drop in the pipe

Figure 7 shows the results of the measurement of the pressure drop ΔP between the two positions of the sampling taps. In the measurements, the valves V_3 and V_4 shown in Figure 6 were replaced by pressure gauges. The solid line in Figure 7 is the pressure drop predicted by Eqs. 8, 9 and $\Delta P = LdP/dz$, and ΔP of the dashed line is obtained with the value of friction factor for laminar Poiseuille flow ($f = 16/Re$) instead of Eq.

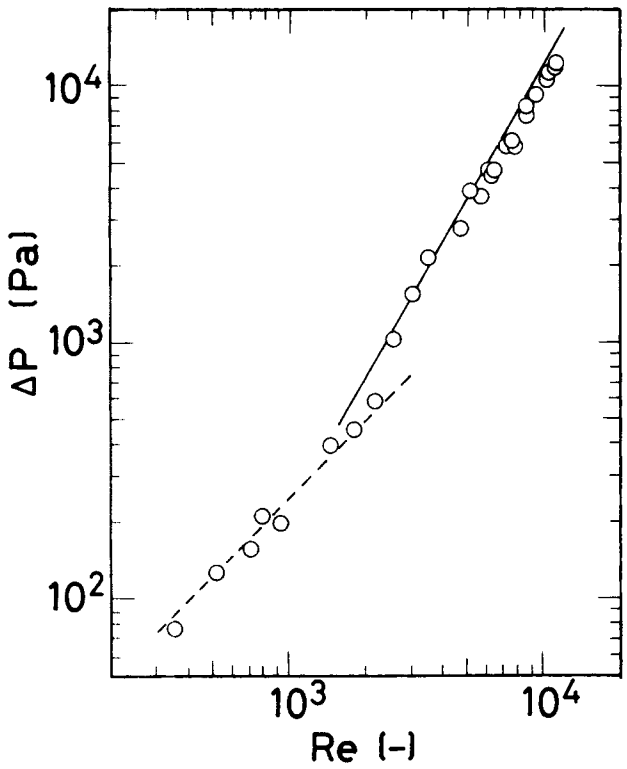

Figure 7. Pressure drop between two sampling taps, ΔP, as a function of the Reynolds number, *Re*.

The solid and dashed lines are the theoretical predictions for incompressible turbulent and laminar fluid flow, respectively.

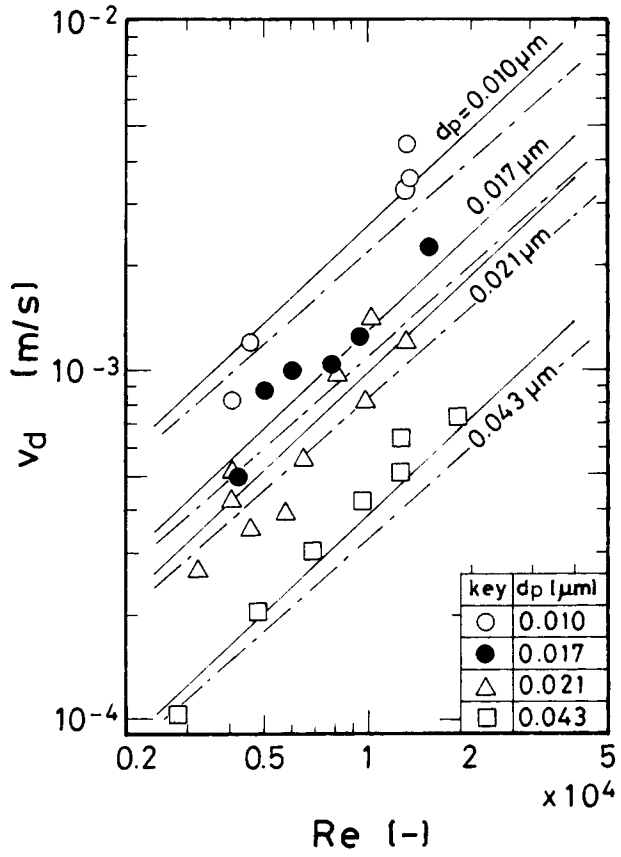

Figure 8. Change in the deposition velocity, v_d, as a function of the Reynolds number, *Re*.

The solid and chain lines are the predictions of Eqs. 13 and 15.

9. As shown in the figure, the measured pressure drops are in good agreement with the prediction for incompressible fluid flows. Consequently, the governing equations for air flow described in the section on theoretical analysis in which compressibility of air is neglected are applicable in the range of this study.

Deposition velocity for turbulent flows

The keys in Figure 8 show examples of measured deposition velocities obtained when $Re \geq 10^3$. The solid and chain lines are the values predicted by Eqs. 14 and 16, respectively. The solid lines (present work) are relatively close to the chain lines, the calculation results of the previous equation. However, the deviations between the lines become significant as *Re* becomes large because of the difference in the exponents of *Re*. There is some scatter in the experimental data, which might have been caused by instability in the dilution of the aerosol. The introduction of a generated aerosol into main airstream of a large flow rate (more than 40 times that of the aerosol) without changing the pressure of the aerosol sometimes required a very delicate adjustment of flow rates and pressures in the experimental setup. The dependence of v_d upon *Re* is found to be closer to the solid lines than to the dashed lines. A least-squares regression analysis performed to the data for every particle diameter indicated that the measured values of v_d were proportional to the 1.0th–1.2nd power of *Re*. This slope is even larger than 0.92 which is expected from the present analysis. Nevertheless, agreement of the measurement and the prediction is satisfactory for deposition velocities ranging over more than an order of magnitude.

Figure 9 shows the change in the deposition velocity as a function of the Brownian diffusion coefficient *D*. A regression analysis of the measurement was applied again to show that the values of v_d vary with the 0.60th–0.73rd power of *D*. These values are in reasonable agreement with that of the present analysis, 0.67. The dependence of the deposition velocity on the Brownian diffusion coefficient has not been demonstrated experimentally in previous studies where turbulent pipe flow and micrometer size particles were used, because the deposition investigated there was affected by particle inertia. The experimental evaluation of the dependence of the deposition velocities on Brownian diffusivity obtained here is possible because of the use of the submicron particles.

The measured deposition velocities for $Re \geq 3{,}000$ are compared to the predicted values in Figure 10. The deviation between the keys and the solid line illustrates the difference between the measurement and prediction. The two dashed lines are the values 50% larger or smaller than perfect agreement.

It has been pointed out that the $k-\epsilon$ model fails to predict some flows correctly. Properties of flow computed by the $k-\epsilon$ model are reported to be different from those obtained by direct simulation or those predicted with the fluid momentum equation in the very near wall region (Mansour et al., 1989). However, the applicability of the $k-\epsilon$ model has not been understood for prediction of ultrafine particle deposition. This

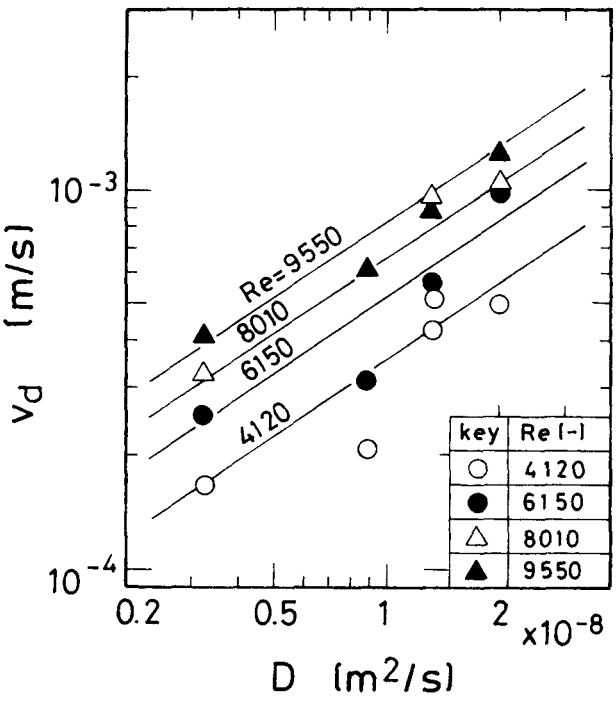

Figure 9. Change in the deposition velocity, v_d, as a function of the Brownian diffusion coefficient, D.

The solid lines are the predictions of Eq. 13.

figure shows that all the experimental results lie between the dashed lines, indicating that the present theoretical analysis can give adequate results for turbulent diffusive deposition of ultrafine aerosol particles.

Figure 11 shows a comparison of the results of the present study with experimental data and theoretical predictions obtained previously for high Schmidt number mass transfer using

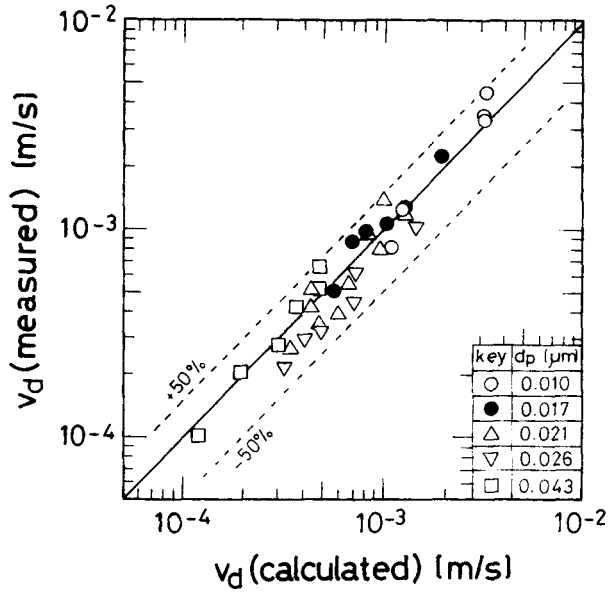

Figure 10. Comparison of the measured and predicted deposition velocities.

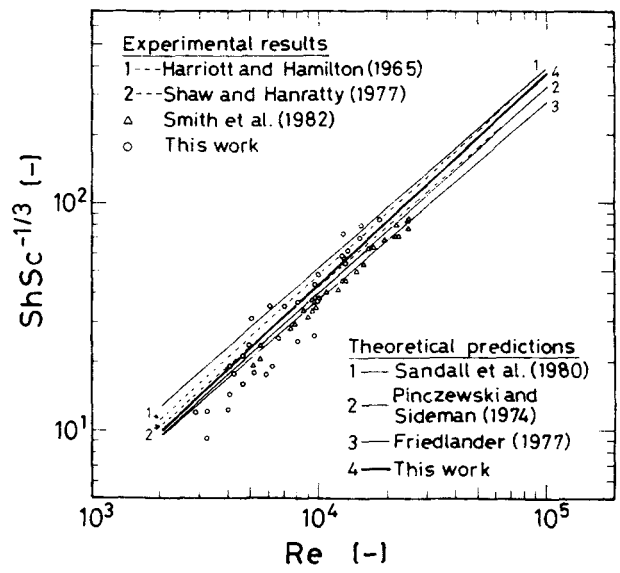

Figure 11. Comparison of the results of the present study with those previously obtained using liquid systems.

liquid systems. Since the results by Smith et al. (1982), Friedlander (1977) and this study indicate that Sh is proportional to $Sc^{1/3}$, the ordinate of the graph is set to $ShSc^{1/3}$ to see the dependence of Sh on Re. The dependence on Sc is slightly different from 1/3 in the theoretical results of Sandall et al. (1980) and Pinczewski and Sideman (1974), and the experimental results of Harriott and Hamilton (1965) and Shaw and Hanratty (1977), so that the values shown in the figure is those for a middle Sc value in the present experimental conditions ($Sc = 1.2 \times 10^3$).

It is clear in this figure that the data and predictions of mass transfer for liquid systems are close to one another and exhibit a dependence very similar to the data of the present measurement. Consequently, the deposition of very fine aerosol particles can be treated in a similar method to mass transfer in single phase systems, which has not been confirmed experimentally so far. Such fine particles as used in this study are considered to have negligible inertia and behave like fluid in turbulent flow. It is also seen in the figure that the calculation line of this study lies within the range of the existing predictions. Although it is not determined which prediction is the most appropriate, the present calculation using the $k-\epsilon$ model also gives satisfactory results in prediction of mass-transfer rates in a turbulent pipe flow.

Deposition velocity for laminar and transitional flows

Figure 12 shows the experimental results for particles 0.017 μm in diameter obtained when Re was varied down to 10^2. The two different keys correspond to the sampling methods described in the section on experimental apparatus and procedure. A difference in the sampling method does not affect the measurement and the experimental results obtained by either method are in good agreement when Re is around 2,000.

The solid line in the figure is the prediction for turbulent diffusive deposition, Eq. 14 and, as previously mentioned, describes the measurement for deposition occurring in tur-

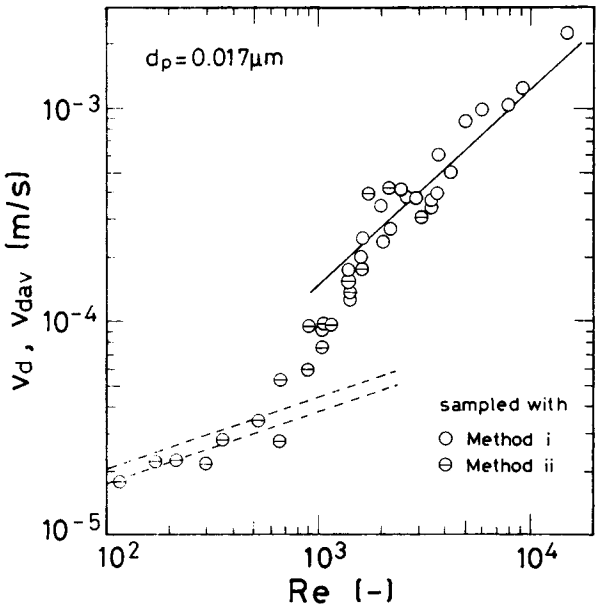

Figure 12. Deposition velocity, v_d, as a function of the Reynolds number, *Re*, for particles 0.017 μm in diameter.

The solid line is the prediction for turbulent diffusive deposition, and the dashed lines are the predictions for deposition in laminar pipe flow.

bulent flows quite well. The measured deposition velocities, however, deviate from the solid line when *Re* is smaller than about 2,000.

The dashed lines in the figure indicates the theoretical average deposition velocity v_{dav} from Eqs. 17-19 and 21. In these calculations, the position of the cross-section over which the distribution of particles was uniform was assumed to be that of the sampling tap at the upstream side or that of the inlet of the test pipe (0.7 m apart from the upstream-side sampling tap). Using these assumptions, the upper and lower dashed lines in the figure were obtained by setting $(z_u, z_d) = (0$ m, 6 m) and (0.7 m, 6.7 m) in Eq. 19, respectively. The two dashed lines are relatively close to each other and both explain the measurement for $Re \lesssim 1{,}000$ well.

The deposition velocities measured when $1{,}000 \lesssim Re \lesssim 2{,}000$ are for transitional flows because they are not explained by the solid nor the dashed lines. Deposition in transitional flows was also found in our previous experimental study where flows in stirred tanks were used (Shimada et al., 1991). The prediction of deposition in transitional flows requires a theoretical description of particle transport in this flow regime, and this is left for future work.

Conclusions

Diffusive deposition of submicron particles from turbulent and transitional pipe flow has been studied theoretically and experimentally, and the following results are obtained.

• The turbulent diffusion coefficient of particles, which is assumed to equal the eddy diffusivity of air, is calculated to be nearly proportional to the third power of the distance from the surface of the pipe wall. When the calculated deposition velocities are presented in terms of dimensionless parameters, the dimensionless deposition rate, *Sh*, is found to be proportional to the 0.92nd power of *Re* and the 0.67th power of *Sc*.

• The measurement of particle concentration in a pipe with $100 \lesssim Re \lesssim 10{,}000$ has clarified the dependence of deposition velocity upon particle size and flow rate. When *Re* is larger than about 3,000, the measured deposition rates are within $\pm 50\%$ of those predicted by the present theoretical analysis and validate the analysis. Deposition occurring in transitional flows has also been observed in the measurements when $1{,}000 \lesssim Re \lesssim 2{,}000$.

Notation

A, b, c = constants
C_c = Cunningham correction factor
C_1, C_2, C_μ = values given by Eq. 7
d_p = particle diameter, m
D = Brownian diffusion coefficient, $m^2 \cdot s^{-1}$
D_E = turbulent diffusion coefficient, $m^2 \cdot s^{-1}$
f = friction factor
f_1, f_2, f_μ = functions defined by Eq. 7
k = turbulent energy, $m^2 \cdot s^{-2}$
K_B' = Brownian coagulation rate function, $m^3 \cdot s^{-1}$
K_T' = turbulent coagulation rate function, $m^3 \cdot s^{-1}$
L = distance between two pipe sections, m
n = particle number concentration, m^{-3}
$\bar{n}, \bar{n}_d, \bar{n}_u$ = average particle number concentration over pipe section, m^{-3}
n_C = particle number concentration at center of pipe, m^{-3}
n_i = initial particle number concentration, m^{-3}
n_0 = uniform particle number concentration at $z = 0$, m^{-3}
P = pressure, Pa
r = radial coordinate, m
R = inner radius of pipe, m
R_t = value given by Eq. 7
Re = Reynolds number $(= 2R\bar{u}/\nu)$
Sc = Schmidt number $(= \nu/D)$
Sc_t = turbulent Schmidt number $(= \nu_t/D_E)$
Sh = Sherwood number $(= 2Rv_d/D)$
t = time, s
T = absolute temperature, K
u = air flow velocity, $m \cdot s^{-1}$
$\bar{u}$ = average air flow velocity over pipe section, $m \cdot s^{-1}$
u_c = air flow velocity at central axis, $m \cdot s^{-1}$
$u*$ = friction velocity, $m \cdot s^{-1}$
v_d = deposition velocity, $m \cdot s^{-1}$
v_{dav} = average deposition velocity, $m \cdot s^{-1}$
y = distance from wall, m
y^+ = dimensionless distance from wall
z, z_d, z_u = axial coordinate, m

Greek letters

β = value given by Eq. 21
$\Delta\bar{n}$ = particle loss in section Δz, m^{-3}
ΔP = pressure drop in pipe, Pa
Δz = differential length in axial direction, m
ϵ = energy dissipation rate, $m^2 \cdot s^{-3}$
κ = Boltzmann constant, $J \cdot K^{-1}$
μ = viscosity of air, Pa·s
ν = kinematic viscosity of air, $m^2 \cdot s^{-1}$
ν_t = eddy kinematic viscosity of air, $m^2 \cdot s^{-1}$
ρ = density of air, $kg \cdot m^{-3}$
$\sigma_k, \sigma_\epsilon$ = values given by Eq. 7

Literature Cited

Beal, S. K., "Deposition of Particles in Turbulent Flow on Channel or Pipe Flows," *Nucl. Sci. Eng.*, **40**, 1 (1970).

Cleaver, J. W., and B. Yates, "A Sub Layer Model for the Deposition of Particles from a Turbulent Flow," *Chem. Eng. Sci.*, **30**, 983 (1975).

Davies, C. N., "Definitive Equation for the Fluid Resistance of Spheres," *Proc. Phys. Soc.*, **57**, 259 (1945).
Davies, C. N., "Deposition of Aerosols from Turbulent Flow through Pipes," *Proc. Roy. Soc. London*, **A289**, 235 (1966).
Fichman, M., C. Gutfinger, and D. Pnueli, "A Model for Turbulent Deposition of Aerosols," *J. Aerosol Sci.*, **19**, 123 (1988).
Forney, L. J., and L. A. Spielman, "Deposition of Coarse Aerosols from Turbulent Flow," *J. Aerosol Sci.*, **5**, 257 (1974).
Friedlander, S. K., *Smoke Dust and Haze*, p. 77, Wiley, New York (1977).
Friedlander, S. K., and H. F. Johnstone, "Deposition of Suspended Particles from Turbulent Gas Streams," *Ind. Eng. Chem.*, **49**, 1151 (1957).
Gormley, P. G., and M. Kennedy, "Diffusion from a Stream Flowing through a Cylindrical Tube," *Proc. R. Ir. Acad.*, **52**, 163 (1949).
Harriott, P., and R. M. Hamilton, "Solid-Liquid Mass Transfer in Turbulent Pipe Flow," *Chem. Eng. Sci.*, **20**, 1073 (1965).
Jones, W. P., and B. E. Launder, "The Prediction of Laminarization with a Two-Equation Model of Turbulence," *Int. J. Heat Mass Transfer*, **15**, 301 (1972).
Kousaka, Y., K. Okuyama, T. Niida, T. Hosokawa, and T. Mimura, "Activation of Ultrafine Particles by Supersaturation in Condensational Process," *Part. Charact.*, **2**, 119 (1985).
Liu, B. Y. H., and T. A. Ilori, "Aerosol Deposition in Turbulent Pipe Flow," *Environ. Sci. Technol.*, **8**, 351 (1974).
Mansour, N. N., J. Kim, and P. Moin, "Near-Wall Turbulence Modeling," *AIAA J.*, **27**, 1068 (1989).
Okuyama, K., Y. Kousaka, and K. Hayashi, "Change in Size Distribution of Ultrafine Aerosol Particles Undergoing Brownian Coagulation," *J. Colloid Interface Sci.*, **101**, 98 (1984).
Okuyama, K., Y. Kousaka, and T. Yoshida, "Turbulent Coagulation of Aerosols in a Pipe Flow," *J. Aerosol Sci.*, **9**, 399 (1978).
Papavergos, P. G., and A. B. Hedley, "Particle Deposition Behaviour from Turbulent Flows," *Chem. Eng. Res. Des.*, **62**, 275 (1984).
Pinczewski, W. V., and S. Sideman, "A Model for Mass (Heat) Transfer in Turbulent Tube Flow. Moderate and High Schmidt (Prandtl) Numbers," *Chem. Eng. Sci.*, **29**, 1969 (1974).
Sandall, O. C., O. T. Hanna, and P. R. Mazet, "A New Theoretical Formula for Turbulent Heat and Mass Transfer with Gases or Liquids in Tube Flow," *Canadian J. Chem. Eng.*, **58**, 443 (1980).
Sehmel, G. A., "Particle Deposition from Turbulent Air Flow," *J. Geophys. Res.*, **75**, 1766 (1970).
Sehmel, G. A., "Particle Eddy Diffusivities and Deposition Velocities for Isothermal Flow and Smooth Surfaces," *J. Aerosol Sci.*, **4**, 125 (1973).
Shaw, D. A., and T. J. Hanratty, "Turbulent Mass Transfer Rates to a Wall for Large Schmidt Numbers," *AIChE J.*, **23**, 28 (1977).
Shimada, M., K. Okuyama, Y. Kousaka, and D. Minamino, "Experimental Study of Aerosol Deposition in Stirred Flow Fields Ranging from Laminar to Turbulent Flows," *J. Chem. Eng. Japan*, **24**, 203 (1991).
Smith, R., M. F. Edwards, and H. Z. Wang, "Pressure Drop and Mass Transfer in Dilute Polymer Solutions in Turbulent Drag-Reducing Pipe Flow," *Int. J. Heat Mass Transfer*, **25**, 1869 (1982).
Wood, N. B., "A Simple Method for the Calculation of Turbulent Deposition to Smooth and Rough Surfaces," *J. Aerosol Sci.*, **12**, 275 (1981).
Yoshioka, N., C. Kanaoka, and H. Emi, "On the Deposition of Aerosol Particles to the Horizontal Pipe Wall from Turbulent Stream," *Kagaku Kogaku*, **36**, 1010 (1972).

Appendix

For monodisperse aerosol particles, the change in particle number concentration with time due to particle coagulation is described as:

$$\frac{dn}{dt} = -(K_B' + K_T')n^2 \tag{A1}$$

where K_B' and K_T' are the Brownian and turbulent coagulation rate functions. K_T' for an aerosol in a turbulent pipe flow is expressed according to our previous investigation (Okuyama et al., 1978) as:

$$K_T' = 0.65 d_p^3 (f\bar{u}^3/2R\nu)^{0.5} \tag{A2}$$

The maximum value of K_T' for the conditions of this study is found at the largest particle size and flow rate ($d_p = 0.043$ μm, $Re = 10{,}000$). The value of K_T' for this case is calculated to be approximately 2×10^{-18} m^3/s. Following Okuyama et al. (1984), the value of K_B' for NaCl particles of 0.01–0.04 μm in diameter is about 10^{-15} m^3/s. Therefore the turbulent coagulation can be neglected in comparison with the Brownian coagulation. Then a solution of Eq. A1 is given as:

$$\frac{n}{n_i} = \frac{1}{1 + K_B' n_i t} \tag{A3}$$

when the particle concentration, n, is equal to the initial concentration, n_i, at the residence time, t, is zero. The maximum residence time of the aerosols in the present measurement is about 23 s for the aerosol flowing at $Re = 100$. The particle coagulation is negligible when n/n_i is nearly equal to 1. Substitution of t and K_B' into Eq. A3 gives the maximum number concentration below which the concentration change of particles is due solely to particle deposition. When $n/n_i \geq 0.99$, $t = 23$ s and $K_B' = 10^{-15}$ m^3/s, the maximum concentration is calculated to be 4.3×10^{11} particles/m^3. This particle number concentration is about 3 or 4 orders higher than that used in this study.

Manuscript received Nov. 5, 1991, and revision received July 20, 1992.